Construction and Building Materials 447 (2024) 138176

Contents lists available at ScienceDirect

Construction and Building Materials

journal homepage: www.elsevier.com/locate/conbuildmat

Experimental study of electroosmosis and (Cl^-) diffusion in fired-clay bricks

Naser Eslami [a,*], Lisbeth M. Ottosen [a], Jorge Feijoo Conde [b], Elisa Franzoni [c], Juan Manuel Paz-Garcia [d]

[a] DTU Sustain, Technical University of Denmark, Denmark
[b] Defense University Centre, Spanish Naval Academy, Spain
[c] Civil, Chemical, Environmental and Materials Engineering, University of Bologna, Italy
[d] Chemical Engineering, University of Malaga, Spain

ARTICLE INFO

Keywords:
Electroosmosis
Electromigration
Effective diffusion coefficient
Chloride
Bricks

ABSTRACT

Electroosmosis (EO) is considered as a base for methods in drying moist masonry. EO and the other transport mechanisms, namely electromigration and diffusion, that can influence EO in the bricks, were studied in four Danish bricks with different manufacturing years and locations. Brick cubes were cut from each brick type and then saturated in NaCl 0.1 M solution. A cell with four electrodes was used to measure the electroosmotic permeability coefficient using a phenomenological approach based on non-equilibrium thermodynamics. The effective diffusion coefficient for chloride and electromigration coefficient were calculated. Results showed that the EO flux obtained in the bricks did not follow either the magnitude of zeta potential or ionic content present in the bricks. It was observed that there was a correlation between the EO coefficient and the porous structure of the brick, especially with the pore connectivity, since the bricks with higher pore connectivity and, therefore, with higher effective diffusion coefficient had a higher electroosmotic coefficient.

1. Introduction

Bricks are among the most important and widely used construction materials for buildings in Denmark and many other countries. Pores in the capillary size range in the bricks are responsible for rising damp in the masonry, leading to poor indoor conditions and the onset of decay mechanisms in the wall. The presence of moisture in masonry walls composed of bricks and mortar joints can strongly influence the behavior of the system, affecting the overall performance of the building: energy consumption, structural response, durability, and service life [1].

Electroosmosis (EO) refers to the phenomenon whereby pore water transport is induced due to the application of an external electric field. EO flow phenomenon serves as the base for a type of technologies applied to fight rising moisture in buildings and construction materials [2,3]. Electroosmotic transport depends on the so-called electroosmotic coefficient, k_e ($m^2V^{-2}s^{-1}$) [4].

The physical explanation behind EO is the interaction between the electric field and the electrical double layer (EDL) that forms at the solid-liquid interface within the porous medium. The EDL is a thin region at the interface between an electrolyte solution and a solid surface, where the electroneutrality does not hold. The origin of the formation of EDL comes from the fact that the surface of the solids is either positively or negatively charged. As a consequence, a thin layer containing an accumulation of ions of the opposite charge of the surface exists near the surface in a sub-micrometer region. When an electric field is applied, it exerts a force on the ions in the diffuse layer, leading to a net fluid motion due to viscous drag. This flow is generally directed from the anode towards the cathode, and its velocity is directly proportional to the applied electric field strength and inversely proportional to the viscosity of the fluid.

Ions' presence can play an essential role for the transport mechanism in porous materials, as they can affect soil's electrical conductivity and zeta potential, further influencing the electrokinetic response [5]. Cameselle and Pena [6] showed the effect of heavy metals on electromigration and EO in relation to soil remediation. In some cases, ions' transport and EO occur in opposite directions. For instance, in case NaCl is present, the Cl^- ions electromigrate against the electro-osmotic flow while Na^+ ions electromigrate in the same direction as EO. Therefore, understanding the quantity of electroosmotic water transport in the

* Corresponding author.
E-mail addresses: naes@dtu.dk (N. Eslami), limo@dtu.dk (L.M. Ottosen), jfeijoo@cud.uvigo.es (J.F. Conde), elisa.franzoni@unibo.it (E. Franzoni), juanma.paz@uma.es (J.M. Paz-Garcia).

https://doi.org/10.1016/j.conbuildmat.2024.138176
Received 2 May 2024; Received in revised form 30 August 2024; Accepted 31 August 2024
Available online 3 September 2024

porous materials necessitates considering other transport mechanisms, such as electromigration and diffusion of the ions inside the porous matrix. The electromigration of ions during electrokinetic remediation was investigated by several researchers [7–10], but the electromigration of ions and the effect of ions transport during the EO water transport has not been studied in detail.

This work aims to study experimentally the influence of other transport mechanisms, such as electromigration and diffusion of ions on EO in the bricks, to provide an understanding of electro-osmotic flow in the masonry and optimize the method based on EO for drying brick masonry. The objective is to determine the correction value of transport coefficients by measuring electroosmotic flow. The apparatus described in [11] was used for this purpose. Experiments were conducted on four different types of bricks to understand how electroosmotic flow varies among them.

2. Materials and methods

2.1. Theoretical considerations

2.1.1. Electroosmotic permeability coefficient

Several theories have been proposed to explain EO and to provide a basis for quantitative predictions of the water flow. The Helmholtz-Smoluchowski (H-S) model is one of the earliest and widely used models to describe EO:

$$k_e = \frac{\zeta \, \mathfrak{E}}{\eta} n \tag{1}$$

where ζ (V) is the zeta potential, η (Pa/s) is the viscosity, n (-) is the porosity, $\mathfrak{E}$ (F/m) is the relative permittivity or dielectric constant and finally k_e ($m^2 \cdot V^{-1} \cdot s^{-1}$) is the coefficient of electroosmotic hydraulic connectivity.

However, in this model, the coefficient for EO permeability (k_e) is dependent on the charge in the shear plane (zeta potential) of the electric double layer, relative permittivity, viscosity of the solution and total porosity and independent of the pore size of the medium. It is assumed that pore radii are relatively large compared to the thickness of the diffuse double layer and that mobile ions are concentrated near the soil-water interface [12]. For heterogeneous materials such as bricks it seems suitable to consider EO in specified volume of material and hereby cover the anisotropy and heterogeneity of the material. This phenomenon can be approached from the point of view of *non-equilibrium thermodynamics*, especially since this approach is independent of the assumption regarding the water transport channels [13]. Based on this, EO is related to phenomenological coefficient, and it can be studied experimentally:

$$J_v = L_{11} \nabla(-P) + L_{12} \nabla(-\emptyset) \tag{2}$$

$$J_q = L_{21} \nabla(-P) + L_{22} \nabla(-\emptyset) \tag{3}$$

Where J_v represents the volume flux, J_q is the charge flux, P is the fluid pressure and Ø is the electrical potential as in [11]. The coefficients L_{11} and L_{22} are direct coefficients, where the flux is directly linked to the force. L_{22} is the factor that relates electric current to the potential gradient, i.e., Ohm's Law. $L_{11}$is the factor of proportionality between solution flow and pressure gradient in the case where no electric field is present. L_{21} is the factor that relates applied pressure and resulting current in case of no electric field. L_{12} is the factor, proportional to applied electric field and volume flow, therefore represents the coefficient for EO (k_e). According to the Onsager's theorem, the phenomenological coefficients (cross coefficients) are equal (L_{12}=L_{21}), which simplifies the calculation of the coupled phenomenon. Then for the coefficient of EO, we have:

$$(L_{12})_{\nabla(-P)=0} = \boldsymbol{J}_V / \nabla(-\emptyset) \tag{4}$$

And for electric conductivity:

$$(L_{22})_{\nabla(-P)=0} = \boldsymbol{J}_q / \nabla(-\emptyset) \tag{5}$$

Effective diffusion coefficient

Chemical transport driven by chemical potential gradient is termed diffusion. The relationship of the parameters is controlled by Fick's Law [4]:

$$J_D = -D_i \frac{\partial c}{\partial x} A \tag{6}$$

Where $D_i$is the diffusion coefficient, A is the cross-section area and $\frac{\partial c}{\partial x}$ is the concentration gradient. It is possible to obtain tabulated values for ideal diffusivities, D_i (m^2/s), of ionic and non-ionic species, in free electrolytes and almost infinite dilution conditions. Chemical species transport through a porous material is slower and more complex due to several reasons, such as a) reduced cross-section area for flow because of the presence of the solid fraction, b) tortuous flow paths around particles, c) influence of electrical force fields caused by the double-layer distributions of charges, and d) osmotic counter flow [14]. The "effective" diffusion coefficient, D_i^{eff}, is used to describe the apparent diffusion coefficient, taking into account these transport hindering factors. Several definitions have been proposed in which the different factors are considered differently [14]. For instance, material properties are suggested by [15] in the relationship between D and D^{eff}

$$D_i^{\text{eff}} = p \frac{\delta}{\tau} D_i \tag{7}$$

Where p is the porosity, τ is the tortuosity and δ is the constrictivity (the influence of narrow pores on ion transport determined by the ratio between the ion and pore diameter [16]). Alternatively, the Bruggeman's correlation, popular for porous media formed by spherical particles, correlates the effective and ideal diffusivities using only the porosity and a fitting parameter β, denoted as the Bruggeman's coefficient [17]:

$$D_i^{\text{eff}} = p^{\beta} D_i \tag{8}$$

In a porous medium, such as a brick sample whose pores have been previously saturated with a solution, the flux of each ion, $\boldsymbol{J}_i$ (mol $m^{-2}s^{-1}$), and the flux of water, $\boldsymbol{J}_w$ (m/s), can be described using the Nernst-Planck equation and considering that water movement through the pore structure is due only to electroosmosis, so the convective term is the electroosmotic ionic transport [18,19]:

$$\boldsymbol{J}_i = \underbrace{-D_i^{\text{eff}} \nabla C_i}_{\text{Diffusion}} \underbrace{-U_i c_i \nabla \phi}_{\text{Electromigration}} \underbrace{-c_i K_{e.o.} \nabla \phi}_{\text{electroosmotic advection}} \quad ; \quad i = 1, \, 2..N \tag{9}$$

$$\boldsymbol{J}_w = -K_{e.o.} \nabla \phi \tag{10}$$

where D_i^{eff} (m^2/s) is the already defined effective diffusion coefficient, c_i (mol/m^3) is the concentration, U_i ($m^2V^{-1}s^{-1}$) is electromigration coefficient, $\nabla\phi$ (V) is the electric potential gradient, and $K_{e.o}$ is the electroosmotic permeability coefficient ($m^2V^{-1}s^{-1}$).

The Nernst-Einstein equation relates diffusion and electromigration coefficients:

$$U_i = \frac{F z_i}{RT} D_i^{\text{eff}} \tag{11}$$

where R is the gas constant (8.3143 J/mol/K), T (K) is the temperature, F is the Faraday constant and z_i is the electric charge.

Assuming that diffusion in the Nernst-Planck equation is very low compared to electromigration and electroosmosis (which is the case in the used EO cell since it is the same solution that is in the pores and the upper chambers), the effective diffusion coefficient of the solution will be:

$$-D_i^{\text{eff}} = \frac{RT}{Fz_i}\left(\frac{J_i}{c_i \nabla \phi} + K_{e.o.}\right) \quad (12)$$

Considering a faradic efficiency of 100 %, the ionic flux and charge density are related as:

$$\mathrm{F}\sum_{i=1}^{N} J_i = I, \quad (13)$$

where I (A/m^2) is the applied current density, so it would be possible to estimate the effective diffusion coefficient of each ion, and therefore characterize porous media.

2.2. Investigated bricks

Four types of bricks from different places in Denmark were chosen for this study: Horsens yellow brick (1850) (also labeled as Ho), Dalum yellow brick (1874–1940) (also labeled as Da), Bispebjerg red brick (1900) (also labeled as Ho) and a normal red brick manufactured recently, labeled as New (Fig. 1). The selection was based on the diversities in localities to represent the traditional Danish bricks. Further research can focus on the effect of production year and manufacturing process on EO in these bricks. A total of 8 cubes having size 3 cm × 3 cm × 3 cm were cut from each brick type. Two of the cubes from each brick type were used in the EO experiments, and the rest were used for the tests related to the physical properties and ion content of the different bricks, i.e., 8 brick cubes in total (2 cubes from each type) were used in the EO experiment. Moreover, one cube with the size of 4 cm × 4 cm × 4 cm was cut from each brick to measure the compressive strength test. The open porosity was calculated as the porosity accessible by water according to UNE-EN 1936:2007, i.e., from the relationship between the weight of the saturated brick in vacuum, the hydrostatic weight, and the dry weight of the material. Capillary suction test was carried out according to UNE-EN 1925:1999, obtaining the water absorption coefficient by capillarity, and capillary porosity was calculated using total water absorption by capillarity at the end of the test. The Mercury Intrusion Porosimetry (MIP) was conducted using a mercury intrusion porosimeter Thermo Fisher Scientific Pascal 140 and 240 using duplicate brick samples having size 1 cm × 1 cm × 2 cm. The zeta potential (ζ) of the bricks was measured on mechanically ground brick powder using a Zetasizer Nano Z, from Malvern Instruments, applying electrophoresis measurement (EPM). For this purpose, 10 g of powder was taken and suspended in 25 ml of distilled water. The particle size distribution test for the brick powder was conducted using a Malvern Mastersizer 2000 and Scirocco-ADA2000 instrument with a measuring range of 0–2 mm. The compressive strength test was conducted using a Matest E161PN173 instrument with a measuring range of 0–250kN according to DS/EN 196–1.

2.3. Preparing brick cubes for EO experiment

Each brick cube was placed in a sample holder specifically designed for the experiment [20], and then it was coated with epoxy resin to cover the four external surface of the brick, which were outside the sample holder. The remaining two opposite faces of the brick cube inside the sample holder were left free of epoxy (Fig. 2). The epoxy coating was used to avoid any outflow of water during the experiment (including evaporation) and hereby to ensure that the water flow occurred only through the matrix of the bricks between the compartments. After drying the resin for 24 hours, the brick cubes were vacuum saturated for 24 hours in a 0.1 M NaCl solution to obtain fully saturated specimens.

Two extra brick cubes were contaminated with NaCl 0.1 M in

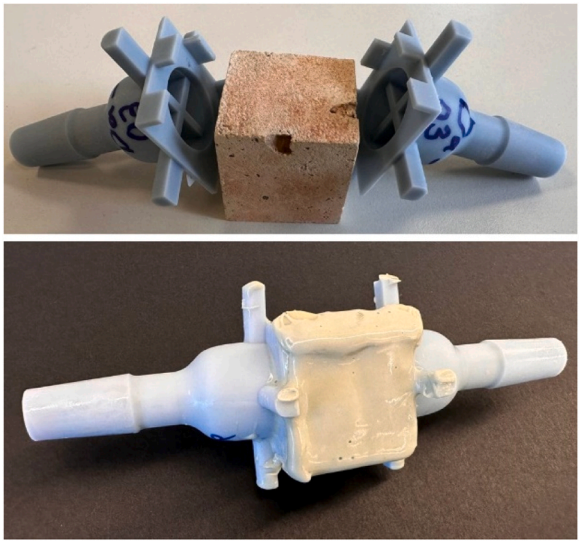

Fig. 2. The brick cubes embedded in the sample holder (upper), and the surface of the bricks coated with epoxy resin (lower).

Fig. 1. Picture of the four bricks used in this study.

vacuum together with the cubes in the sample holders, i.e., under the same condition. These extra specimens were used to measure the pH and conductivity before the experiment, as well as for the ion chromatography (IC) analysis to measure the chloride, sulfate, and nitrate concentration. For this analysis, 5.0 g of brick powder were suspended in 12.5 g distilled water and the suspension was shaken for 8 hours. The pH and conductivity were measured in the suspension, using a pH-meter and a conductivity-meter respectively, after a few minutes of settling. The suspensions were then filtered for the IC analysis (Dionex ICS-100 instrument). After the EO experiment, the same measurements were performed on those brick specimens. It should be noted that in this study, the bricks first were contaminated with NaCl solution, then the measurement of ion content was conducted- before the experiment. This means that the initial ion content of the bricks was not measured before the contamination. Therefore, the results in this paper represent only the ion content after contamination.

2.4. The electroosmotic set-up

The EO cell used (Fig. 3) was developed in [11] for measuring EO coefficients in clays and later adapted to bricks [20]. This cell is designed based on the phenomenological approach in Eq. (8). The cell is a four-electrode cell with two working electrodes in the lower chambers and two reference electrodes placed in the upper chambers. The sample holder, with the brick cube inside, was placed between two symmetrical parts.

Two copper wires were used as working electrodes and Ag/AgCl were used as reference electrodes to measure the potential gradient over the brick sample.

The two chambers at each side of the brick were separated by a porous glass plate with glass beads on top of it to hinder the pH changes from the electrode processes from reaching the upper chambers. The lower chambers were filled with 1.0 M $CuCl_2$ solution until it reached the level of glass plate. The upper chambers were filled with NaCl 0.1 M solution (the same solution used to contaminate the brick samples) until the cell was completely filled and the solution reached into half of the capillary tube. Two capillary tubes, with the diameter of 0.35 mm, were placed on the top of each of the upper chambers to observe and measure the water flow.

Any bubbles were removed from the cell and all the openings were closed and checked to avoid leaking from the cell. Then, the setup was left for 30 minutes to ensure that there was no movement of water in the capillary tube when no electrical potential gradient was applied. When the level of the solution in the capillary tube was stable for at least 30 minutes, the electric potential difference was applied.

When an electric field is applied to a moist porous material, electrolysis occurs at the electrodes when electrons are transferred from the conductive material to the pore fluid:

$$\text{Anode}: H_2O \rightarrow +\frac{1}{2}O_{2(g)} + 2e^- \quad (14)$$

$$\text{Cathode: } 2H_2O + 2e^- \rightarrow 2OH^- + H_{2(g)} \quad (15)$$

In case of acidic or basic water, the reactions that occur at the electrode interface are slightly different [21]. Water electrolysis leads to hydrogen and oxygen formation, solvent (water) reaction, and the production of protons and hydroxide ions, both with high ionic mobility. Consequently, during water electrolysis, it's challenging to determine if the observed flow is due to overpressures or purely electroosmotic phenomena. Water electrolysis reactions can be avoided by favoring conditions for alternative electrode reactions, such as using copper electrodes in moderately acidic or neutral environments with moderately concentrated Cu^{2+} ion solutions.

$$\text{Anode}: \quad Cu^0 \rightarrow Cu^{2+} + 2e^- \quad (16)$$

$$\text{Cathode}: \quad Cu^{2+} + 2e^- \rightarrow Cu^0 \quad (17)$$

2.5. Experimental procedure

New Ag/AgCl electrodes for each EO experiment were prepared according to the following procedure: two Ag wires with a diameter of 1 mm and length of 12 cm were coated with epoxy resin so only the very tip of the wire was open. Hereafter the electrodes were immersed in a diluted solution of HNO_3 for 60 minutes then rinsed in distilled water. The electrodes were then electrochemically prepared following [22,23], i.e., a solution of 1 M KCl was prepared, and the Ag wires were galvanostatically charged at 2 mA for 15 minutes (against a platinum wire as cathode). The half-cell reaction at the anode is as follows:

$$Ag + Cl^- \rightarrow AgCl + e^- \quad (18)$$

By this procedure, the surface of the tip of the electrodes was covered by a layer of Ag/AgCl. After preparation, the potential of the electrodes was measured with respect to another standard Ag/AgCl reference electrode using a 0.1 M HCl solution. When not in use, the two electrodes were stored in a 0.1 M KCl solution.

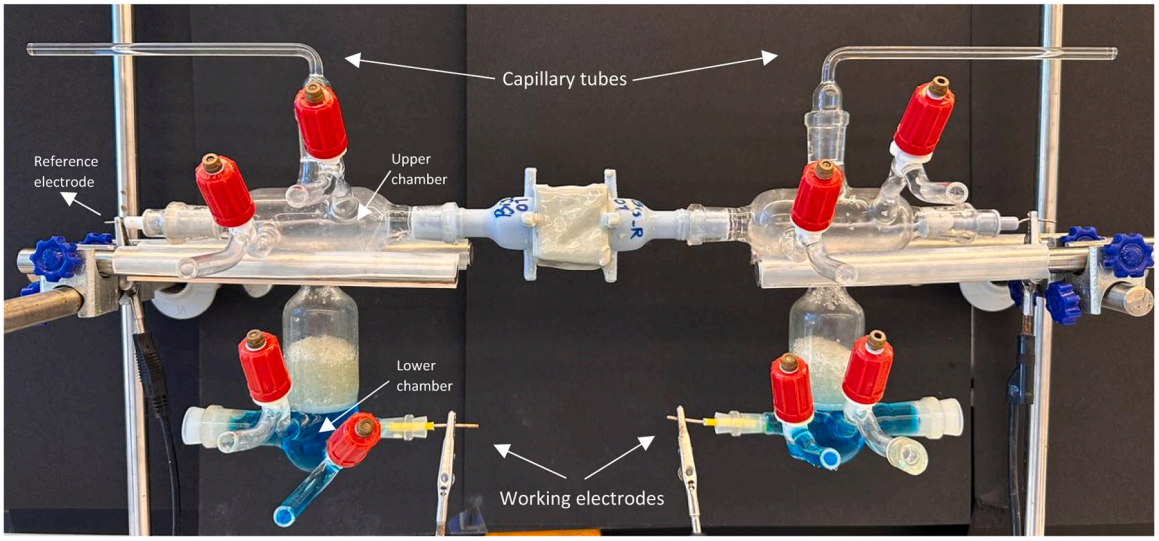

Fig. 3. The EO cell used to measure the EO flow in brick cubes (coated in epoxy resin) placed in the middle of two double electrode chambers.

The EO experiment for each brick specimen was conducted with a constant voltage in four different levels: 60, 50, 40 and 30 V and the current (mA) was recorded for each of the voltage levels. A total of 6 changes in polarity were conducted for each voltage. The time for the water flow was measured for every 2 cm of the capillary tube (until 10 cm). The time of the solution in the capillary tube to reach a certain distance, the potential difference recorded at the Ag/AgCl electrodes, and the dimensions of the bricks were used to calculate the water flow rate and the EO permeability coefficient in the experiment using Eq. (10). The average values for each two replicates were calculated to measure the water flow rate in each brick type, considering that in each of them the measurements were made 6 times (for each of the polarity changes made).

To describe the ion transport in the bricks, the effective diffusion coefficients (D_i^{eff}) were studied. For this, Cl^- was chosen as base for three reasons: it is an ion with high ionic mobility [16], it is not influenced by adsorption or precipitation/dissolution reactions in the concentration range of this investigation, and it has the opposite electromigration direction compared to the EO flow. Eq. (12) was chosen to describe D_i^{eff} of Cl^- since it combines electromigration and electroosmotic fluxes. The ionic flux for chloride (J_{Cl}), in four range of electrical potential, was obtained using the following equation:

$$J_{Cl^-} = \frac{I}{F \cdot A} \tag{19}$$

where I is the electric current, F the Faraday constant and A the cross section of the bricks to get the transport of the moles of the species (here Cl^-) in square meter of the brick in the unit of time. The ionic concentration (c_i) was calculated using the ion content obtained from IC analysis, the molecular weight of Cl^-, the porosity and the density of the brick to get the moles of the Cl^- per cubic meter of the brick. The EO coefficient (k_{eo}) was the same L_{12} calculated in Eq. (4).

3. Results and discussion

3.1. Brick properties

Table 1 shows the physical properties and zeta potential of the bricks. It can be seen that both yellow bricks (Dalum and Horsens) have the highest porosity values for both water accessible porosity and capillary porosity, as well as the highest capillary coefficients. This indicates that they present a higher pore volume, which allows a faster capillary suction of water than that reached by the red bricks assessed, i.e. New and Bispebjerg (Fig. 4). These red bricks have similar values of porosity, which are lower than those showed by the yellow bricks mentioned above, however, there is a difference between the two red bricks since Bispebjerg, despite having a slightly lower water accessible porosity than the New brick, has a slightly higher capillary porosity. This indicates that capillary transport in this brick is more significant than in the New brick.

The pore connectivity of the four bricks analyzed is good, since without applying vacuum they are able to reach water saturation degrees through capillary absorption higher than 95 %, being higher in the Bispebjerg and Dalum bricks. These factors of porosity and connectivity between pores, according to the model proposed by [15], have a direct influence on effective diffusion.

Table 1
Mechanical properties and characteristics of the bricks.

	New	Bispebjerg	Dalum	Horsens
Water accessible porosity (%)	13.2	12.9	19.1	18.4
Capillary porosity (%)	5.8	6.3	9.5	9.3
Saturation degree by capillary suction (%)	96.2	98.0	97.4	96.9
Capillary coefficient ($kg/m^2s^{0.5}$)	0.427	0.460	0.732	0.686
Dry Density (g/cm^3)	2.1	2.2	2.0	2.1
Zeta potential (mV)	−21.73	−26.6	−27.9	−29.5
Compressive strength (MPa)	21.93	20.99	10.48	25.13

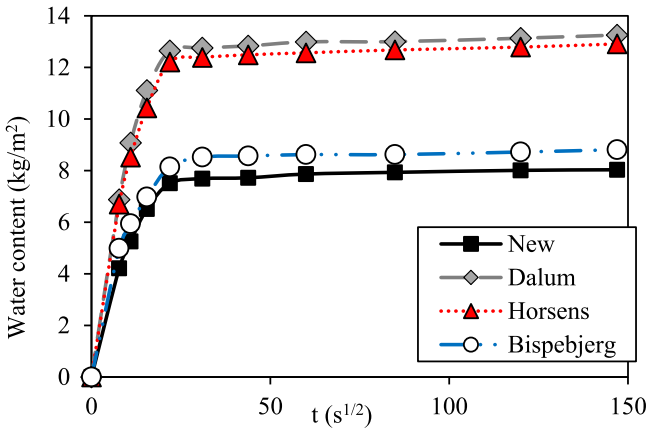

Fig. 4. Water content per surface unit area as a function of time during the capillary absorption test for the four types of bricks assessed.

The pore size distribution curves obtained by mercury intrusion porosimetry are reported in Fig. 5. It can be observed that the total open porosity of the bricks is consistent with the values obtained by water absorption test (Table 1).

With respect to the zeta potential, in all the bricks the value is negative, which indicates that the electroosmotic transport must occur from the anode to the cathode. In addition, it can be seen that the bricks with the highest zeta potential (in absolute value) are the Horsens and Dalum bricks.

According to the H-S model for EO (1), both porosity and zeta potential have a direct impact on the value of the electroosmotic permeability coefficient, so that the higher the value of the two parameters, the higher the expected value of the electroosmotic coefficient. According to the model suggested by [15], there is a direct relationship between the porosity and effective diffusion, meaning that the higher porosity could result in a higher effective diffusion coefficient.

Results for MIP test shows that the distribution of pores in the New brick is in the range of 0.1–10 μm which is the greatest range compared to other bricks, which indicates that the New brick possesses larger pores. The pores in the Dalum bricks range from 0.2–0.8 μm which is the lowest pore range compared to the other bricks (Fig. 5). In this regard, the range for pore size distribution of the bricks follows the order of New>Horsens>Bispebjerg>Dalum. It was seen that the accessible porosity of mercury for Dalum brick was higher than the other bricks while the Bispebjerg brick had the lowest specific pore volume. It was seen that the Dalum brick had the most narrow pores between the bricks.

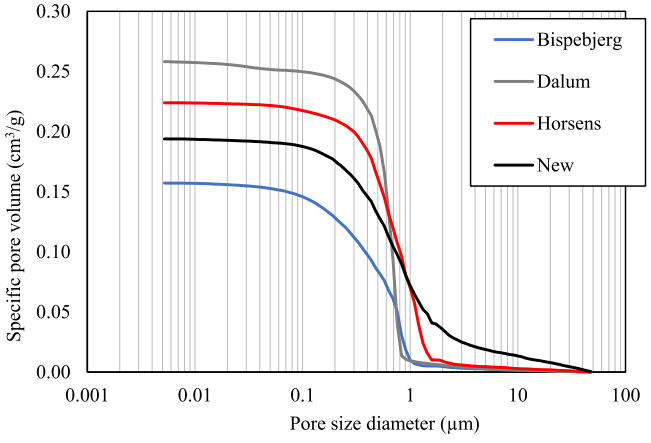

Fig. 5. Pore size distribution curves of the four bricks.

Fig. 6 represents the particle size distribution of the brick powder samples used in measuring the zeta potential, IC and pH values. The particle size ranges from 0.6–400 μm for all the bricks.

The initial ionic content of the different bricks (Table 2) shows that chloride was the major ion in all cases, followed by sulfate in the case of Dalum and New bricks, and nitrate in the case of Horsens and Bispebjerg bricks. The chloride ion content was much higher in Bispebjerg and Horsens bricks. The presence of ions in the bricks influences the measurement of conductivity and ionic strength, both parameters that can influence the electroosmotic process. The higher the ionic content of a material (i.e., its ionic strength), the lower the thickness of the double layer and the lower the efficacy of the electroosmotic flow [24]. In this sense, it can be seen that the conductivity and ionic strength values (considering only the content of chlorides, sulfates and nitrates) are higher in the Horsens and Bispebjerg bricks.

3.2. pH in the bricks before and after EO experiments

The pH influences the electrical conductivity, e.g. in soil, through the distribution of H^+ and OH^- [25]. It also changes the zeta potential [5, 26], which is expected to have an impact on the EO flow. Therefore, it is critically important to stabilize the pH to measure the EO permeability coefficient. Fig. 7 shows the pH of the bricks before and after the EO experiments. The changes in pH were minor. This implies that the used cell successfully hinders major pH changes in the bricks. Furthermore, it was also observed that the pH of the solution in the chambers did not change from before to after the experiments. Thus, the results from the EO cell are not considered influenced by pH changes. The pH can affect the chemical equilibrium in the interface between the solid particle surface and the pore electrolyte. Namely, the pH may affect the magnitude of the surface charge and the composition of the diffuse layer [27]. Therefore, the EO coefficient is expected to be dependent on the pH value of the pore solution.

3.3. Electroosmotic water flow

Fig. 8 shows the time required to cause the displacement of the water, through the capillary tube, under different applied potentials. It can be seen that regardless of the brick evaluated, the higher the voltage applied the faster the movement of water, which takes place from the anode to the cathode due to the negative zeta potential of these materials. This fact is in accordance with [28], and is logical if we considered that the higher the voltage applied, the higher the current flowing (Fig. 9a), keeping the resistance of the brick at a similar value (Fig. 9b). Both aspects indicate that a greater ionic mobilization is taking place.

Comparing bricks, the movement of water is faster in the Dalum brick, which had a high water accessible porosity, even though the current flow through it is one of the lowest. In this brick, the water flow advances at a constant speed until it reaches 10 cm, showing a linear relationship between displacement and time, which could be ascribed to the fact that the pores of this brick are very similar in size, being concentrated mostly in the range 0.2–0.8 μm (Fig. 5). In the other three bricks, the electroosmotic flow process slows down as the water flow advances through the capillary tube. For this reason, the trend line shown in Fig. 8 for each of these three bricks, regardless the voltage applied, shows a logarithmic shape. Comparing the speed of the process in these bricks, it can be seen that this is faster in Bispebjerg followed by the New and Horsens bricks, which show a similar behaviour. This fact shows that the accessible porosity is not the only factor affecting the electroosmotic flow rate, since Horsens exhibits a higher porosity than the other two bricks, and the ranking of the EO flow speeds in Fig. 8 does not follow that of the total porosity in Fig. 5. Moreover, it can be noticed that the influence of voltage increase on the EO flow is different for the different bricks, increasing according to the following order: Dalum< Bispebjerg <New<Horsens. In particular, a decrease in the voltage applied from 60 V to 30 V slows down the flow especially in bricks New and Horsens and this cannot be explained based on their total porosity, while it can be noticed that these two bricks exhibit a significant amount of large pores (r > 1 μm), which are not present in the others. In addition to this, the influence of other parameters such as ionic strength and zeta potential must be analysed.

At the end of the test, the total ionic content inside each of the bricks, as well as the values of ionic strength and conductivity, shows lower

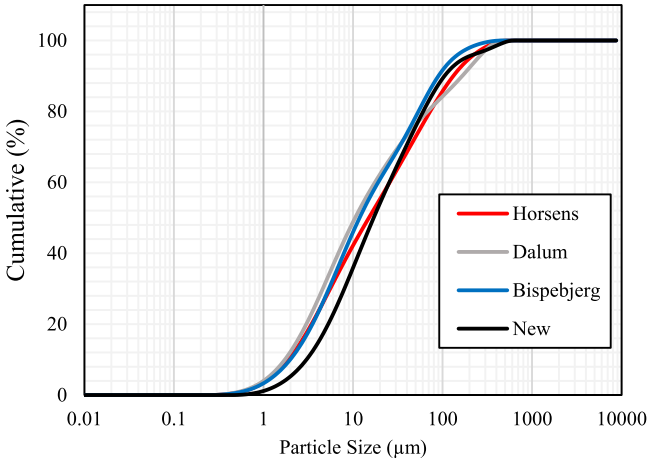

Fig. 6. Particle size distribution of brick powder.

Table 2
Ionic content, ionic strength, and conductivity of the brick samples before and after the EO experiment.

		New	Bispebjerg	Dalum	Horsens
Cl^- (mg/kg)	Before	614	1780	888	1350
	After	562	1565	371	1230
	Desalination efficacy (%)	8.47	12.08	58.22	8.89
SO_4^{2-} (mg/kg)	Before	100	23	70	57
	After	122	234	88	41
	Desalination efficacy (%)	−22.00	−917.39	−25.71	28.07
NO_3^- (mg/kg)	Before	24	108	24	703
	After	5	257	4	915
	Desalination efficacy (%)	79.17	−137.96	83.33	−30.16
Ionic strength	Before	0.010	0.026	0.013	0.025
	After	0.009	0.027	0.006	0.025
Conductivity (mS/cm)	Before	0.84	1.12	1.30	1.86
	After	0.75	2.18	0.89	2.25

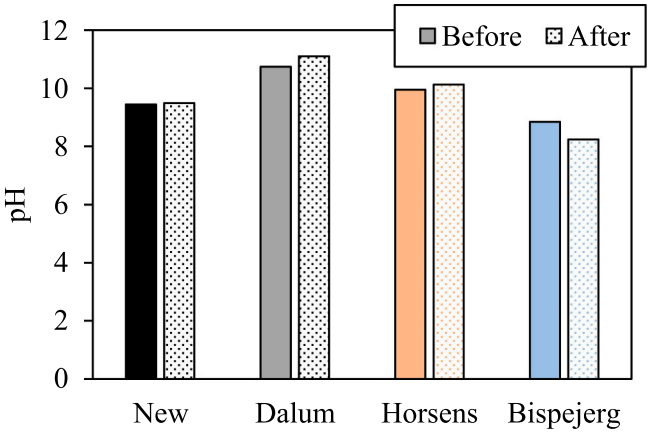

Fig. 7. pH level of the bricks before and after the experiment.

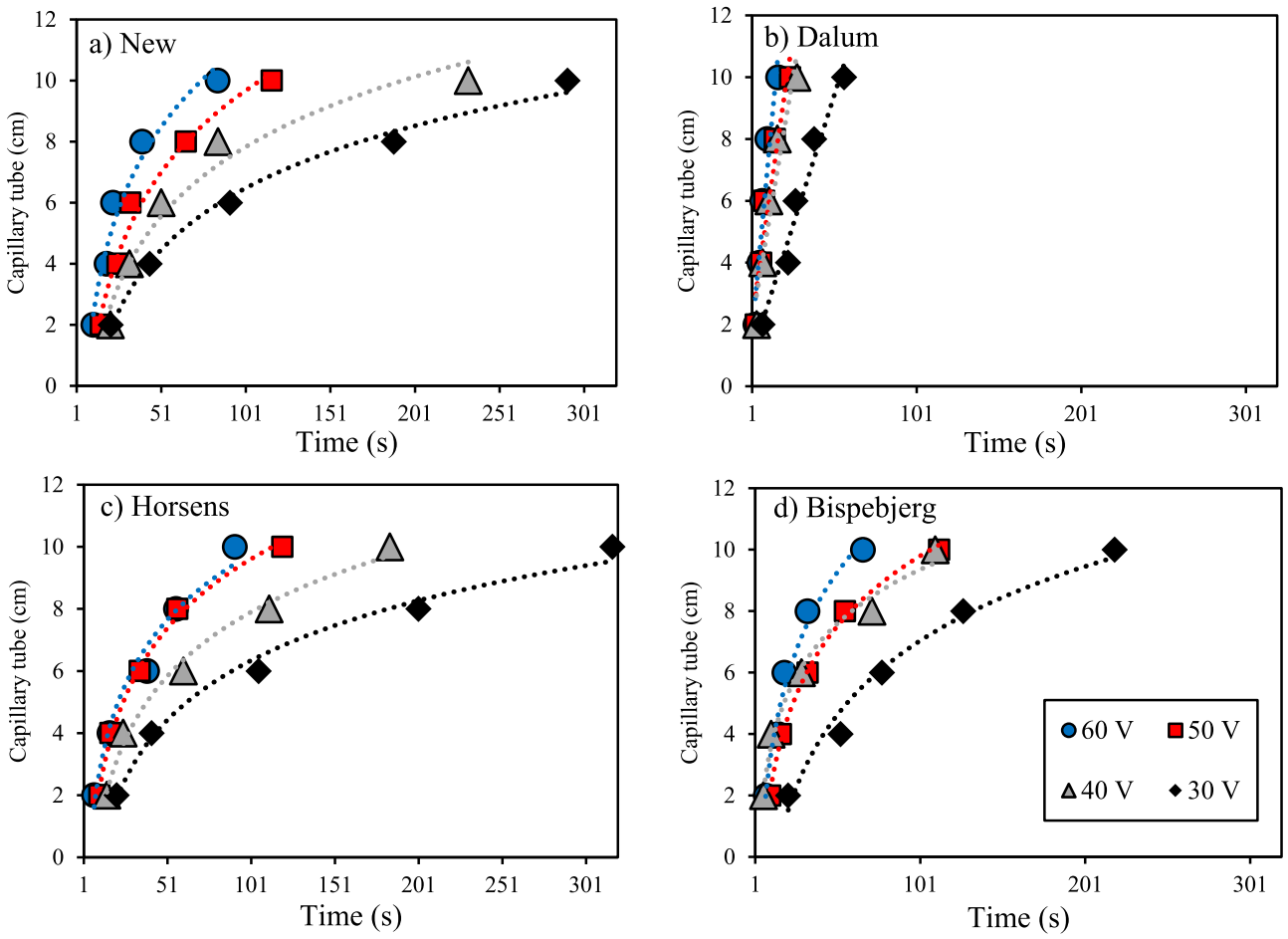

Fig. 8. Time required for the movement of water to travel certain distances within the capillary tube when different voltages are applied. The trend line that best fits each case is also shown.

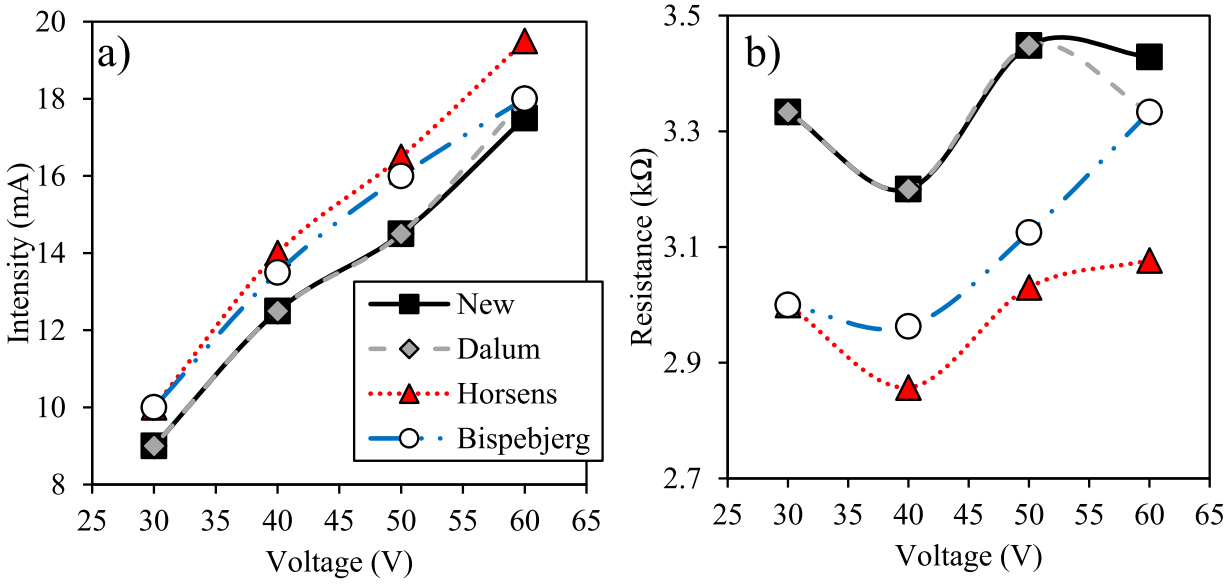

Fig. 9. Evolution of the current intensity (a) and resistance (b) of each of the bricks analyzed for each of the voltages applied.

values for the Dalum brick and New brick (Table 2). This fact would be favorable to the electroosmotic flow since the lower the ionic strength, the greater the thickness of the electrical double layer. On the opposite side are the Horsens and Bispebjerg bricks, which have a greater ionic content, which should slow down the electroosmotic process. These hypotheses do not strictly agree with the experimental data obtained since the process is faster in Dalum and Bispebjerg bricks.

Fig. 8 shows that EO transport slows down with time. As the cell was

working in a constant voltage, the decrease of EO was related to the decrease of the ionic current. The decrease in the ionic current was a consequence of the increase in the resistivity. As shown before, the pH was constant, so the resistivity was not related to the pH, but a change in the salt concentration in the pore solution.

The relationship between ζ -potential and EO permeability is defined in H-S Eq. (1), and this model states that the higher the value for ζ -potential the higher the EO flow. Thus, according to this, the Horsens brick should be expected to have the highest EO flow, while the New brick should be expected to have the lowest EO flow rate since it had the lowest value for the ζ -potential (Table 1). As seen from Fig. 8, this is not confirmed in the experiments, showing that other brick properties than the ζ -potential have a greater impact on the EO flow rate.

The only property that seems to maintain a direct relationship with what was observed in the experiments is the pore connectivity (measured through the saturation degree of capillary absorption, Table 1). The pore connectivity and the presence of ink bottle pores should be further investigated to confirm this.

3.4. Electroosmotic permeability coefficient

The EO permeability coefficient (L_{12}) (as phenomenological coefficient) was calculated using Eq. (4) for the four electrical potential differences. The volume flow rate (J_v) was calculated considering the time of water flow in 10 cm of the capillary tube, the water volume transported in the specific time and the dimension of the brick sample. The slope of the linear relations in Fig. 10 is the EO coefficient in accordance with Eq. (4).

In general, it can be seen that in all cases there is a linear fit between the potential gradient and Jv, obtaining correlation coefficients (R^2) greater than 0.90 (Fig. 9 and Table 3). It is seen that the EO coefficient (L_{12}) in the Dalum brick was considerably higher than in the other bricks (Table 3). The New and Horsens brick have similar EO coefficients with overlapping lines.

Comparing the order of brick EO coefficients (Table 2) and measured brick characteristics (Table 1 and Figs. 4 and 5), a relationship between pore connectivity and EO coefficients is observed. Furthermore, it was seen that the brick with a pore size range of 0.2–0.6 μm, had the highest value of L_{12}. However, this correlation does not appear for other bricks such as New and Horsens bricks. The relationship/influence of the other parameters is not so direct and they probably play a joint influence. As abovementioned, there is no link between the ζ -potential and the EO coefficient. The Dalum brick with the highest EO coefficient had the highest open porosity and the capillary suction was similar to the Horsens and faster than the two other bricks, whereas the Bispebjerg brick with the second highest EO coefficient had the lowest open porosity and slowest capillary suction. Thus, there is not one of these characteristics, that singles out the other in relation to determining the EO coefficient, or there are other more important factors that must be taken into account.

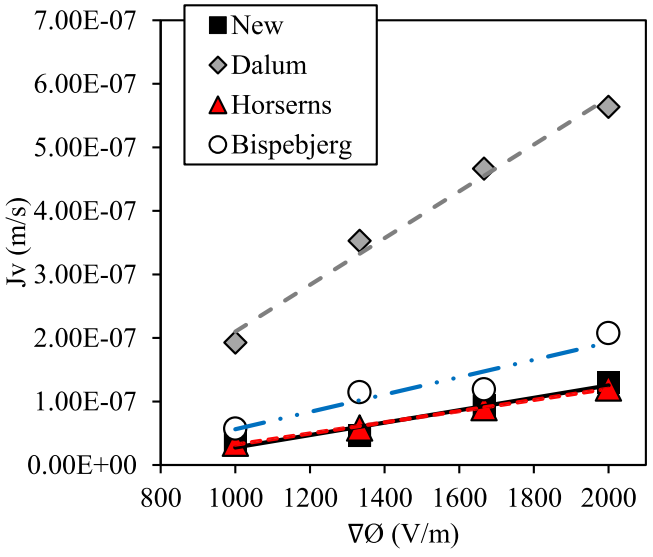

Fig. 10. Average volume flow rate (Jv) versus voltage gradient ∇Ø, considering the time of water flow in 10 cm of the capillary tube.

Table 3
The electroosmotic permeability coefficients for the brick cubes at four different electric potential differences.

Bricks	L_{12} (m^2/V s)	R^2	linear fit equation
New	9.77E−11	0.95	Jv = 9.77E−11·∇Ø − 7.01E−08
Dalum	3.68E−10	0.99	Jv = 3.68E−10·∇Ø − 1.58E−07
Horsens	8.80E−11	1.00	Jv = 8.80E−11·∇Ø − 5.60E−08
Bispebjerg	1.37E−10	0.90	Jv = 1.37E−10·∇Ø − 8.03E−08

3.5. The effective diffusion coefficient of chloride ($D_{Cl^-}^{eff}$)

The calculated D_{Cl}^{eff} for the bricks at four different applied potential differences is shown in Fig. 11. It can be seen that the $D_{Cl^-}^{eff}$ was relatively constant for every brick regardless the applied potential difference, which was in accordance with what expected. The average values for $D_{Cl^-}^{eff}$ for each of the bricks (Fig. 12) showed that the Dalum brick has the highest $D_{Cl^-}^{eff}$ (around 1.27×10^{-11} $m^2\cdot s^{-1}$) and the Horsens brick the lowest with a value of 5.31×10^{-12} $m^2\cdot s^{-1}$. This value is still much lower than the value for Cl^- at infinite diluted solution (2.03×10^{-09} $m^2\cdot s^{-1}$ [4]). This is in accordance with expectations due to the affecting parameters such as porosity and tortuosity in the brick that reduce the diffusion of ions. This result also agrees with the desalination efficiency achieved at the end of the test, which is indicative of the ease with which anions move through the porous structure (Table 2). The highest extraction percentages are achieved in Dalum brick followed by Bispebjerg brick.

When comparing the results for D_i^{eff} and the EO permeability coefficient, a direct correlation was found, i.e., the brick with highest EO coefficient had the highest D_i^{eff} and the one with the lowest EO coefficient had the lowest D_i^{eff}. These results show the correlation of EO in bricks and the diffusion of ions such as chlorides. The more the EO in the bricks, the more the movement of ions. According to the theory of EO, the hydrated ions carry the water molecules in response to the electric field. The results in this study proved the relation of ions movement and electroosmotic water flow in the bricks.

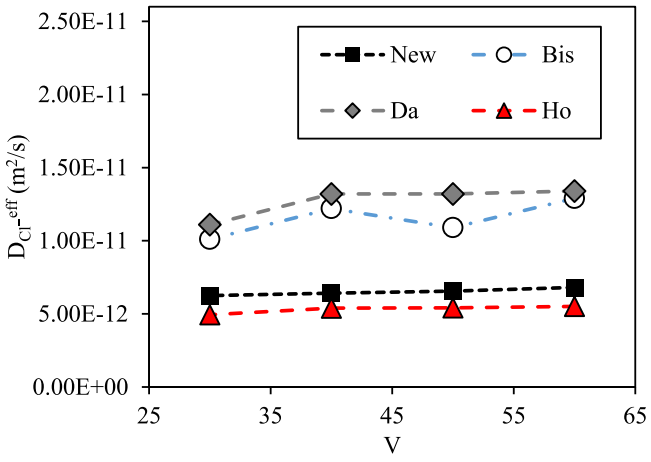

Fig. 11. Effective diffusion coefficients for Cl in the bricks at four different applied voltages.

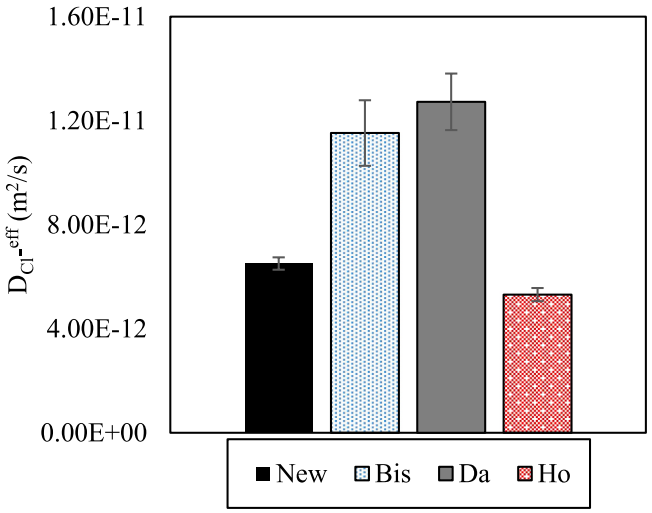

Fig. 12. The average values of the D_i^{eff} for Chloride in the four bricks.

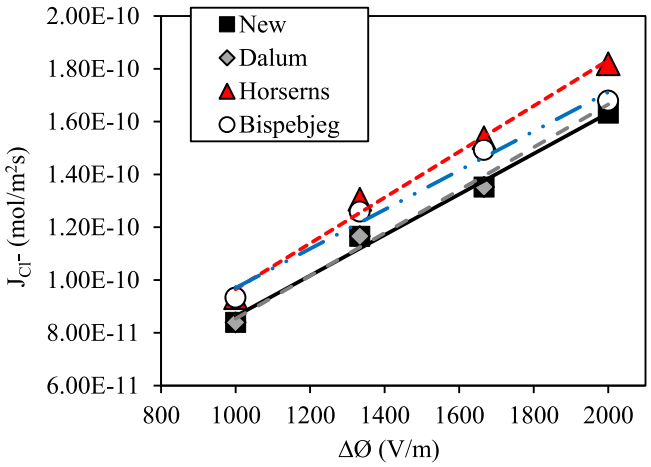

Fig. 13. the ionic flux in the bricks in four different potential gradients during the experiment.

Fig. 13 represents the diffusive flux as a function of the electric potential gradient and shows that the Cl^- flow rate has an almost linear relationship with the applied potential gradient. For instance, in all four brick, the diffusive flux was 1×10^{-4} (mol/m^2·s) under the application of 60 V. This value was reduced to 5×10^{-5} (mol/m^2·s) when the applied electric potential difference reduced to 30 V. The ionic flux in the bricks is based on the current density since the charge is carried by the ions. Therefore, it was expected that the ionic flux values are according to the magnitude of the electric current, which was recorded after applying the electric potential. The slight fluctuation in the ionic flux is related to the small differences in the electric current recorded for each brick cube replicates. The results indicate for both ionic and electroosmotic flow rate that the magnitude of electrical potential is crucially important.

4. Conclusions

An electroosmotic water flow was generated in four different brick types, three of them extracted from old buildings (1850–1900) in different regions of Denmark and the fourth brick was new. The EO in the bricks was measured, and the electroosmotic permeability coefficient was calculated using a phenomenological approach based on non-equilibrium. Effective diffusion coefficients were also calculated. Analyzing the results obtained in this study, the main conclusions drawn are as follows:

1) The influence of the pore structure of bricks on the electroosmotic flow is demonstrated. Bricks with higher pore connectivity and with narrower pores within the range of capillary pores facilitate the electroosmotic flow.

2) The higher pore connectivity allows to reach a higher effective diffusion, finding a direct relationship between the effective diffusion of the main anion present in the brick and the electroosmotic coefficient that characterizes it.

3) The influence of the pore structure of a brick on the efficiency of the electroosmotic process is greater than that exerted by other parameters such as the zeta potential or the ionic strength of the solution present in it, which is in contrast with the mathematical models for describing electroosmosis in soils such as Helmholtz-Smoluchowski model. The existence of narrower capillary pores and within a smaller dispersion range, i.e. pores with similar sizes, favor faster electroosmotic transport and does not slow down the rate with the distance traveled by the water.

Summarizing, in order to predict the efficiency of the electroosmotic process, in construction materials such as bricks the ease with which the ions can move through the pore structure must be taken into account (effective diffusion coefficient), which will depend on factors such as porosity, tortuosity and constrictivity. However, the influence of other parameters such as the zeta potential of the material or the initial ionic content should not be ruled out

CRediT authorship contribution statement

Naser Eslami: Writing – review & editing, Writing – original draft. **Lisbeth M.Ottosen:** Writing – review & editing, Supervision. **Jorge Feiijo Conde:** Writing – review & editing, Supervision. **Elisa Franzoni:** Writing – review & editing. **Juan Manuel Paz.Garcia:** Writing – review & editing, Supervision.

Declaration of Competing Interest

The authors declare that they have no known competing financial interests or personal relationships that could have appeared to influence the work reported in this paper.

Data availability

Data will be made available on request.

Acknowledgments

Grundejernes Investerings Fond and Realdania are acknowledged for the financial support to this study. Special acknowledgment is given to the professional support provided by the Defense University Center at the Spanish Naval Academy (CUD-ENM).

References

[1] R. Ramirez, B. Ghiassi, P. Pineda, P.B. Lourenço, Simulation of moisture transport in fired-clay brick masonry structures accounting for interfacial phenomena, Build Environ vol. 228 (2023) 109838, https://doi.org/10.1016/j.buildenv.2022.109838.
[2] E. Franzoni, State-of-the-art on methods for reducing rising damp in masonry, J Cult Herit vol. 31 (2018) S3–S9, https://doi.org/10.1016/J.CULHER.2018.04.001.
[3] L.M. Ottosen, I. Rörig-DalgaardDrying brick masonry by electro-osmosis," 7th International Masonry Conference, vol. 2, no. October, 2006 .
[4] J.K. Mitchell, Fundamentals of Soil Behavior, 2nd editio, Wiley, New York, 1993.
[5] L.M. Vane, G.M. Zang, "Effect of aqueous phase properties on clay particle zeta potential and electro-osmotic permeability: implications for electro-kinetic soil remediation processes,", J Hazard Mater vol. 55 (1–3) (1997) 1–22, https://doi.org/10.1016/S0304-3894(97)00010-1.
[6] C. Cameselle, A. Pena, Enhanced electromigration and electro-osmosis for the remediation of an agricultural soil contaminated with multiple heavy metals, Process Safety and Environmental Protection vol. 104 (2016) 209–217, https://doi.org/10.1016/j.psep.2016.09.002.

[7] J.M. Paz-Garcia, B. Johannesson, L.M. Ottosen, A.N. Alshawabkeh, A.B. Ribeiro, J. M. Rodriguez-Maroto, Modeling of electrokinetic desalination of bricks, Electrochim Acta vol. 86 (2012) 213–222, https://doi.org/10.1016/j.electacta.2012.05.132.
[8] L.M. Ottosen, I.V. Christensen, Electrokinetic desalination of sandstones for NaCl removal - Test of different clay poultices at the electrodes, Electrochim Acta vol. 86 (2012) 192–202, https://doi.org/10.1016/j.electacta.2012.06.005.
[9] J. Feijoo, L.M. Ottosen, O. Matyscak, R. Fort, Electrokinetic desalination of a farmhouse applying a proton pump approach. First in situ experience, Constr Build Mater vol. 243 (2020) 118308, https://doi.org/10.1016/j.conbuildmat.2020.118308.
[10] C. Cameselle, A. Pena, Enhanced electromigration and electro-osmosis for the remediation of an agricultural soil contaminated with multiple heavy metals, Process Safety and Environmental Protection vol. 104 (2016) 209–217, https://doi.org/10.1016/j.psep.2016.09.002.
[11] S. Laursen, Laboratory investigation of electroosmosis in bentonites and natural clays, Canadian Geotechnical Journal vol. 34 (5) (1997) 664–671, https://doi.org/10.1139/cgj-34-5-664.
[12] A. Asadi, B.B.K. Huat, H. Nahazanan, H.A. Keykhah, Electrochemical science theory of electroosmosis in soil, Int. J. Electrochem. Sci vol. 8 (2013) 1016–1025.
[13] A.K. Vijh, J.P. Novak, A new theoretical approach to electroosmotic dewatering (EOD) based on non-equilibrium thermodynamics, Drying Technology vol. 15 (2) (1997) 699–709, https://doi.org/10.1080/07373939708917255.
[14] J.K. Mitchell, Fundamentals of Soil Behavior, 2nd editio, Wiley, New York, 1993.
[15] O. Truc, J.P. Ollivier, L.O. Nilsson, Numerical simulation of multi-species transport through saturated concrete during a migration test - MsDiff code, Cem Concr Res vol. 30 (10) (2000) 1581–1592, https://doi.org/10.1016/S0008-8846(00)00305-7.
[16] I. Rörig-Dalgaard, L.M. Ottosen, K.K. Hansen, Diffusion and electromigration in clay bricks influenced by differences in the pore system resulting from firing, Constr Build Mater vol. 27 (1) (2012) 390–397, https://doi.org/10.1016/j.conbuildmat.2011.07.031.
[17] B. Tjaden, S.J. Cooper, D.J. Brett, D. Kramer, P.R. Shearing, On the origin and application of the Bruggeman correlation for analysing transport phenomena in electrochemical systems, Curr Opin Chem Eng vol. 12 (2016) 44–51, https://doi.org/10.1016/j.coche.2016.02.006.
[18] F. thomas, Fuller, N. John, Harb, Electrochemical Engineering, First. New Jersy, John Wiley & Sons, 2018.
[19] J.M. Paz-Garcia, B. Johannesson, L.M. Ottosen, A.B. Ribeiro, J.M. Rodriguez-Maroto, Modeling of electric double-layers including chemical reaction effects, Electrochim Acta vol. 150 (2014) 263–268, https://doi.org/10.1016/J.ELECTACTA.2014.10.056.
[20] L.M.O.Naser Eslami, Elisa Franzoni, Juanma Paz Garcia, Jorge feijoo, "Measuring electroosmotic permeability coefficient in single bricks,", Submitted to the Jurnal (2024).
[21] E. Zoulias, E. Varkaraki, N. Lymberopoulos, C.N. Christodoulou, G.N. Karagiorgis, A review on alkaline water electrolysis, Tcjst vol. 4 (2) (2004) 41–71.
[22] H. Gu, D.N. Bennion, Diffusion and charge transfer parameters for the Ag / AgCl electrode,", J Electrochem Soc vol. 124 (9) (1977) 1364–1370, https://doi.org/10.1149/1.2133655.
[23] D. Tao, L. Jiang, M. Jin, A method of preparation of Ag/AgCl chloride selective electrode,", J. Wuhan Univ. Technol. Mater. Sci. Edition vol. 33 (4) (2018) 767–771, https://doi.org/10.1007/s11595-018-1890-0.
[24] R.J. Hunter, zeta potential in colloid science, Academic Press, Sydney, 1981.
[25] J. Chen, S.R. A-abed, and L. Murdoch, "Cation transport and partitioning during a field test of electroosmosis cation exchange capacity of the test site soil ranged which was then exchanged and adsorbed The and adsorption resulted in the decrease of the exchangeable," vol. 35, no. 12, pp. 3841–3851, 1999.
[26] Y. Yukselen, A. Kaya, "Zeta potential of kaolinite in the presence of alkali, alkaline earth and hydrolyzable metal ions,", Water Air Soil Pollut vol. 145 (1–4) (2003) 155–168, https://doi.org/10.1023/A:1023684213383.
[27] J.M. Paz-Garcia, B. Johannesson, L.M. Ottosen, A.B. Ribeiro, J.M. Rodriguez-Maroto, Modeling of electric double-layers including chemical reaction effects, Electrochim Acta vol. 150 (2014), https://doi.org/10.1016/j.electacta.2014.10.056.
[28] L. Bertolini, L. Coppola, M. Gastaldi, E. Redaelli, Electroosmotic transport in porous construction materials and dehumidification of masonry, Constr Build Mater vol. 23 (1) (2009) 254–263, https://doi.org/10.1016/J.CONBUILDMAT.2007.12.013.